

Astral microtubules control redistribution of dynein at the cell cortex to facilitate spindle positioning

Mihoko A Tame¹, Jonne A Raaijmakers¹, Bram van den Broek¹, Arne Lindqvist², Kees Jalink¹, and René H Medema^{1*}

¹Division of Cell Biology; The Netherlands Cancer Institute; Amsterdam, The Netherlands; ²Department of Cell and Molecular Biology; Karolinska Institutet; Stockholm, Sweden

Keywords: dynein, spindle orientation, micropattern, microtubules, mitosis

Cytoplasmic dynein is recruited to the cell cortex in early mitosis, where it can generate pulling forces on astral microtubules to position the mitotic spindle. Recent work has shown that dynein displays a dynamic asymmetric cortical localization, and that dynein recruitment is negatively regulated by spindle pole-proximity. This results in oscillating dynein recruitment to opposite sides of the cortex to center the mitotic spindle. However, although the centrosome-derived signal that promotes displacement of dynein has been identified, it is currently unknown how dynein is re-recruited to the cortex once it has been displaced. Here we show that re-recruitment of cortical dynein requires astral microtubules. We find that microtubules are necessary for the sustained localized enrichment of dynein at the cortex. Furthermore, we show that stabilization of astral microtubules causes spindle misorientation, followed by mispositioning of dynein at the cortex. Thus, our results demonstrate the importance of astral microtubules in the dynamic regulation of cortical dynein recruitment in mitosis.

Introduction

Proper control of the cell division plane orientation is a critical feature ensuring normal cell division and development. The positioning of the mitotic spindle plays a crucial role in this process, as it defines the cell division axis and the position of the cleavage furrow.^{1,2} Failure to properly position the spindle can be deleterious to organisms and is implicated in causing aneuploidy, developmental defects, or cancer.³⁻⁵

The mitotic spindle is composed of dynamic microtubules that grow and shrink through the addition and removal of tubulin dimers, respectively.⁶ This dynamic behavior of microtubules allows them to search in intracellular space and to interact with organelles, diverse cellular structures, and the boundaries of the cell.⁷⁻⁹ Astral microtubules are nucleated from the spindle poles in radial arrays toward the cell peripheral space and probe the cell cortex for anchor sites. Control of spindle positioning is achieved through pulling forces exerted on astral microtubules generated by cortically deposited microtubule minus-end-directed motor activity.¹⁰⁻¹²

In many of the systems utilized for the study of mitotic spindle positioning, including yeast,¹³⁻¹⁵ *C. elegans* zygotes,¹⁶⁻¹⁸ mouse skin progenitors,¹⁹ as well as cultured mammalian cells,^{20,21} the spindle orientation pathways converge on the evolutionarily highly conserved multi-subunit motor complex, cytoplasmic dynein 1 (hereafter referred to as dynein). The dynein motor complex interacts

with several additional accessory and adaptor proteins, including the dynactin complex, which is essential for proper localization and activation of the dynein complex.²²⁻²⁴ The minus-end-directed motor activity resides in the homodimer of 2 dynein heavy chains (DHCs), each comprising 6 AAA ATPase motor domains that bind and hydrolyse ATPs and produce step-like motility with their microtubule binding “stalk” domains.^{23,25} Dynein anchored at the cortex is thought to drive spindle movement by “walking” toward the minus-ends of astral microtubules.²⁶⁻²⁸

The regulation of spindle positioning is well studied in yeast, where dynein plays a crucial role in pulling the nucleus into the bud neck between the mother and daughter cells in mitosis. A number of recent studies support for an active microtubule-mediated delivery process of dynein to the cortical docking factor.²⁹ Loss of the cortical dynein anchor, Num1, leads to the accumulation of dynein at plus-ends of astral microtubules,³⁰ whereas dynein mutations that disrupts astral MT plus-end localization leads to reduction in cortical dynein.³¹ Moreover, high-resolution live microscopy of yeast expressing fluorescently tagged dynein have allowed direct observations of dynein offloading from microtubule plus-ends to the cortex.³² A similar observation of a microtubule-dependent 2-step cortical dynein delivery process was made in fission yeast, where dynein localizes to the cortex to facilitate meiotic nuclear oscillations.³³

In vertebrate systems, dynein-dynactin interacts with an evolutionarily conserved protein complex at the cell cortex, which

*Correspondence to: René H Medema; Email: r.medema@nki.nl
Submitted: 01/17/2014; Accepted: 01/28/2014; Published Online: 02/10/2014
<http://dx.doi.org/10.4161/cc.28031>

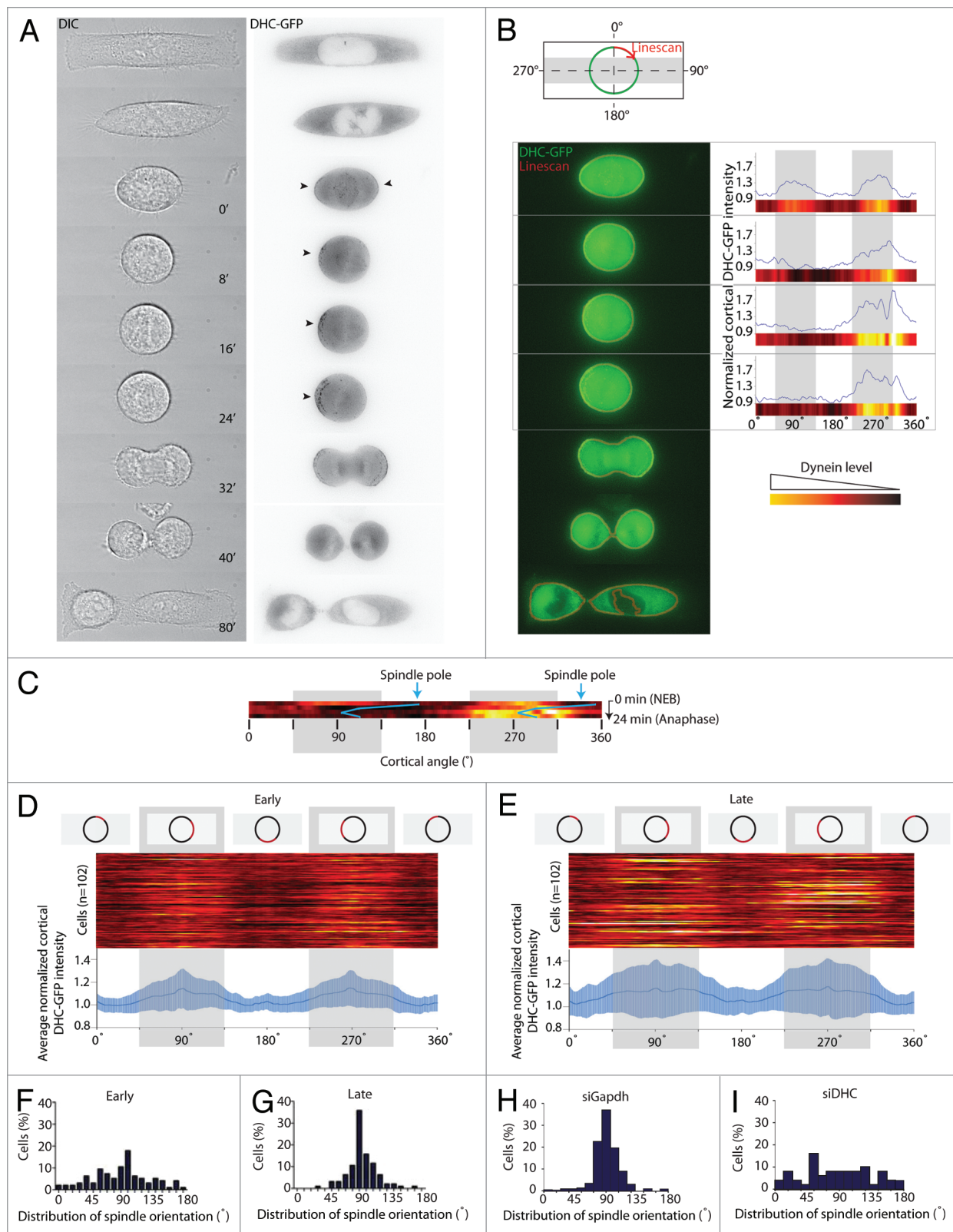


Figure 1. For figure legend, see page 1164.

is distinct from the yeast counterpart and is comprised of $G\alpha$ /LGN/NuMA ($G\alpha$ /GPR-1/2/Lin-5 in *C. elegans*).^{17,20,34,35} This protein complex provides the anchor sites for dynein at the cortex,

from where it is thought to generate pulling forces on the mitotic spindle by capturing astral microtubules and subsequently exerting minus-end-directed motility. Kiyomitsu and Cheeseman

Figure 1 (See previous page). Regulated spindle orientation of micropatterned cells depends on cortical dynein. **(A)** Fluorescence live cell images of a micropatterned HeLa cell stably expressing DHC-GFP. Images are maximum projections of 7 z-slices, taken every 8 min. 0' indicates the first frame acquired after NEB. **(B)** Left: Schematic (top) and an example (bottom) of the cortical DHC-GFP linescan method. The starting position of the linescan is indicated with a red arrow and moves in a clockwise direction around the cortex with a linescan width of 5 pixels. Right: The relative cortical dynein enrichment level is determined by the fluorescence intensity of each cortical angle point normalized to the modal value of all measured cortical intensity values. The normalized intensity values are further converted into a heat map (below each plot). The color code assigning the normalized GFP intensity values is shown on the bottom right. Grey shaded areas in the graphs indicate the preferential spindle orientation angles of control cells relative to the rectangular micropattern, as quantified in **Figure 1G and H**. **(C)** Kymograph of cortical dynein intensity heatmap from the example cell in **(A)**. The angles of the mitotic spindle relative to the shape are plotted at corresponding time points (blue line). **(D and E)** Heatmaps of DHC-GFP in early (first or second frame after NEB) and late (last frame in metaphase) mitotic time points, respectively (n = 102). The averaged intensity values of all heat maps with standard deviations are plotted in a graph (below heat maps). **(F and G)** The spindle angles of the cells used for the analysis in **(D and E)** measured at the corresponding time points, respectively. **(H and I)** Spindle angles in siGAPDH (left) and siDHC (right) treated U2OS cells co-expressing GFP-tubulin and H2B-RFP. Measurements were done in the last time point acquired in metaphase.

(2012) have shown that in mammalian cells, cortical dynein behaves dynamically throughout mitosis, mediating the oscillatory movement of the spindle until it is centered in the middle of the cell. Dynein forms an asymmetric cortical crescent over the spindle pole farthest away from the cell cortex. As the spindle approaches toward the dynein crescent, this dynein population disappears and reappears on the opposite cortical site. Two distinct cell intrinsic signals were identified that mediate this dynein behavior. The chromosome-derived Ran-GTP gradient inhibits LGN–NuMA localization to the cortex, causing the polarized distribution of dynein. Furthermore, the spindle pole-localized kinase Plk1 was identified as a negative regulator of dynein–NuMA interaction, which explains the asymmetric enrichment of dynein. More recently, the major cell cycle regulator cyclin-dependent kinase 1 (CDK1) was identified as another negative regulator of dynein at the cortex, revealing an LGN-independent cortical targeting mechanism of dynein in anaphase, when Cdk1 activity declines.^{36,37} Thus, depending on the cell cycle stage, distinct signaling pathways confer temporal and spatial regulation of dynein.³⁸

In addition to such cell intrinsic cues, emerging evidence also indicates that extrinsic cues from the extracellular matrix contribute to spindle positioning in cultured mammalian cells. Apparently non-polarized in vitro cultured cells exhibit regulated spindle orientation when their adhesion geometry is constrained by the usage of adhesive micropatterns.^{39,40} It was proposed that the extracellular matrix controls actin structure and dynamics at the membrane, which, in turn, impacts on the orientation of the mitotic spindle.^{39,41} Consistently, a number of factors that localize to and regulate cortical actin networks, such as MISP,^{42,43} LIM kinase,⁴⁴ Cdc42,⁴⁵ and PI(3)K⁴⁶ are found to be required for regulated spindle orientation. Although a full picture has yet to emerge, these findings support the idea that a combination of cell-intrinsic and -extrinsic factors mediates spindle orientation in cultured mammalian cells.

Here, we dissect the contributions of these distinct signals by direct observation of dynein at the cortex in cultured cells on micropatterns. Using this experimental setup, we find that the initial cortical localization of dynein is determined by cell external cues and is dictated by the adhesion geometry of the cell. However, in the later stages of mitosis, sustained localized enrichment of dynein at the cortex depends on the presence of microtubules. Moreover, we show that spindle misorientation causes mispositioning of dynein at the cortex. Thus, these

findings demonstrate the importance of astral microtubules in the dynamic regulation of cortical dynein recruitment in mitosis.

Results

Enrichment of dynein at cortical target sites precedes spindle orientation

It has previously been established that adhesion geometry of cultured mammalian cells can dictate the axis of cell division. Cells grown on rectangular micropatterns preferentially orient their mitotic spindle along the long axis of the rectangle.^{39,40} However, whether dynein mediates the rotational spindle movement in cells undergoing mitosis under such geometric constraints has never been directly shown. Visualizing dynein localization to the cell cortex in living cells grown on these micropattern would provide critical insights into dynein's function. For this purpose, we set up fluorescence live-cell imaging experiments using micropatterned HeLa cells stably expressing a bacteria artificial chromosome encoding GFP-tagged mouse dynein heavy chain (DHC-GFP;⁴⁷). Seven focal slide images were acquired every 8 minutes, which allowed us to determine cortical dynein dynamics with good spatiotemporal resolution (**Fig. 1A**). In order to obtain a qualitative read-out for cortical dynein localization and enrichment over time, we generated a macro for image analysis that converts relative cortical DHC-GFP intensities into a heat-map of 360 pixels corresponding to the 360° circumference of a rounded-up mitotic cell (**Fig. 1B**). Using this macro, we found that dynein enrichment at the cortex occurred at early prometaphase and coincided with the first or second time frame acquired (0–8 min) after nuclear envelope breakdown (NEB). At this early phase of mitosis, cortical dynein was symmetrically enriched at 2 opposing sides of the cell (**Fig. 1A–C**). Only later, as cells progressed further through prometaphase and metaphase, dynein became asymmetrically enriched, occasionally switching its cortical enrichment site as described previously (**Fig. 1A–C**; ref. 20). Most importantly, throughout mitosis, cortical dynein enrichment was restricted to cortical sites that are proximal to the short edge of the rectangular micropattern (45°–135° and/or 225°–315°) (**Fig. 1D and E**). In contrast, the mitotic spindle assumed random orientations relative to the geometry of the micropattern immediately after NEB (**Fig. 1C and F**). Whenever the mitotic spindle was initially misoriented, we observed quick and directed rotational movements in prometaphase/metaphase until the spindle was positioned along the long axis of the shape

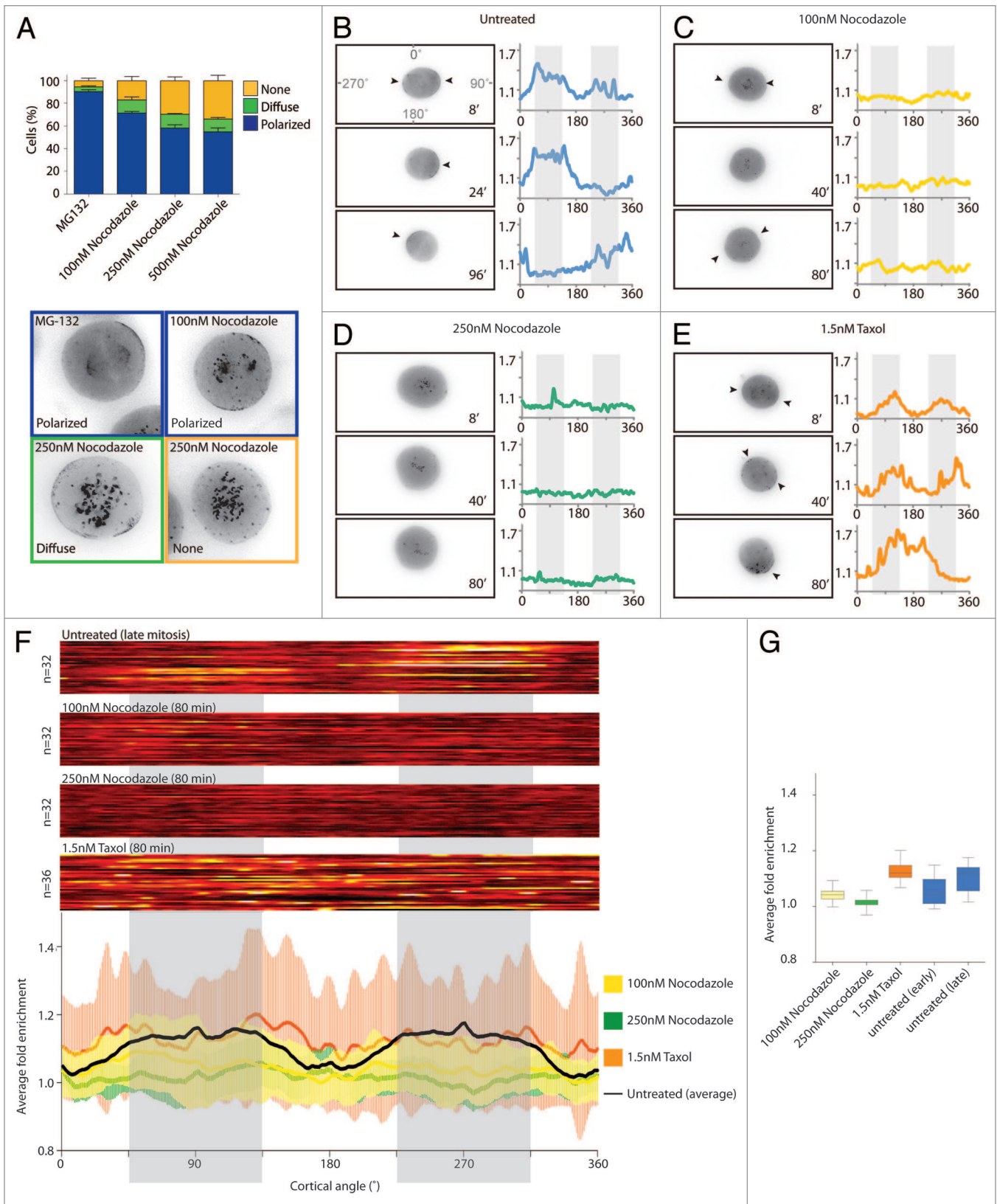


Figure 2. For figure legend, see page 1166.

Figure 2 (See previous page). Cortical dynein enrichment depends on the stability of the mitotic spindle. **(A)** Asynchronous cells were treated for 1 h with the indicated drugs and subsequently scored for the presence of cortical dynein within 2 h. Dynein localization was categorized as polarized, diffuse, and absent (none). Representative images of each category are shown below. Brightness and contrast of images are not scaled equally. Error bars represent SD of 3 independent experiments. **(B)** Relative cortical DHC-GFP intensity level of a control untreated HeLa cell at the 3 indicated time points after mitotic entry. The graphs (right) depict the relative fold enrichment (y-axis) of DHC-GFP at each cortical angle position (x-axis), determined with the same method as described in **Figure 1**. **(C–E)** Time-lapse images and corresponding DHC-GFP enrichment graphs of cells that entered mitosis in the presence of 100 nM or 250 nM nocodazole, and 1.5 nM taxol, respectively. Black arrowheads in the images indicate cortical enrichment sites. Grey shaded areas in the graphs indicate the preferential spindle orientation angles of control cells relative to the rectangular micropattern, as quantified in **Figure 1G**. **(F)** Heatmaps (top) and quantification (bottom) of cortical DHC-GFP enrichment obtained from the experiments shown in figures **(A–D)** at indicated time points. **(G)** Quantification of average DHC-GFP enrichment in **(F)** plotted as a box plot.

(Fig. 1C and G; Video S1). Thus, cortical dynein recruitment precedes spindle positioning. These results suggest that the initial cortical localization of dynein is determined by cell external cues dictated by the adhesion geometry of the cell.

Cortical dynein controls spindle positioning

We next tested whether dynein is required for proper spindle orientation. For this, we analyzed the orientation of the mitotic spindle in cells stably co-expressing H2B-GFP and mCherry-tubulin by fluorescence live-cell imaging. In control cells transfected with GAPDH siRNA, the spindle was preferentially oriented along the long axis of the shape (Fig. 1H, Video S2). Depletion of DHC by siRNA resulted in a large number of cells displaying severe spindle defects with unfocused spindle poles as described in previous reports.^{24,48,49} Nonetheless, the presence of a fraction of cells with bipolar spindles (60%; data not shown) allowed us to analyze spindle orientation in this subpopulation of DHC-depleted cells. Consistent with a role of dynein in spindle orientation, DHC knockdown lead to a severe spindle misorientation phenotype, with no preferential spindle orientation along the long axis of the shape (Fig. 1I; Video S3). Furthermore, we specifically mislocalized the cortical pool of dynein by siRNA-mediated depletion of the cortical dynein targeting factor LGN^{20,50} in the DHC-GFP-expressing cells. As reported earlier, LGN RNAi resulted in loss of cortical dynein localization, with no other observable defects in kinetochore (KT), spindle pole, and spindle localization of dynein (Fig. S1A and B). Similar to DHC knockdown, LGN knockdown resulted in random spindle orientation (Fig. S1C). Taken together, these data indicate that regulated spindle orientation in cells undergoing cell divisions under geometric constraints is mediated by cortically localized dynein.

Local enrichment of cortical dynein depends on the stability of spindle microtubules

As dynein presents a dynamic behavior from prometaphase to metaphase, we next set out to examine how the dynamic redistribution of dynein at the cortex is regulated. It has previously been shown that both the centrosome-associated kinase Plk1 as well as the chromosome-derived Ran gradient negatively regulates recruitment of dynein at the cortex, mediating displacement of dynein from specific cortical areas.²⁰ This allows repositioning of the spindle and, as such, facilitates centering of the spindle in the mitotic cell. However, displacement of dynein must be associated with recruitment of dynein to sites that are (no longer) in the vicinity of the spindle poles or chromosomes. Possibly, this is a simple consequence of stabilization of dynein at cortical regions where negative regulators are not present. Alternatively, dynein

targeting might involve active delivery process via astral microtubules to promote localized enrichment at the cell cortex.

To test the contribution of astral microtubules on cortical dynein localization, we subjected DHC-GFP-expressing HeLa cells to a range of concentrations of spindle microtubule de-stabilizing agent, nocodazole (Fig. 2A). In MG132-arrested control cells, most cells displayed a polarized enrichment of cortical dynein. Upon nocodazole treatment, a large fraction of cells still maintained dynein at the cortex. However, with increasing concentration of nocodazole, an increasing fraction of cells lost dynein from the cell cortex (Fig. 2A). In control cells, only a small fraction of cells were devoid of cortical dynein (5%), whereas the cortical dynein-negative fraction increased more than 3-fold (17%) and 6-fold (30%) in 100 nM and 250 nM nocodazole-treated populations, respectively. A further increase in nocodazole concentration (500 nM) did not lead to a dramatically enhanced effect than at 250 nM nocodazole (34%). Consistent with these observations, analysis of spindle structure by cell fixation and tubulin staining showed that astral microtubules were severely affected at 100 nM nocodazole, whereas all microtubules were completely de-polymerized at a nocodazole concentration of 250 nM (Fig. S2A).

In order to examine this in more detail, we performed live-cell imaging to analyze the effect of nocodazole treatment on cortical dynein enrichment over time. When cells entered mitosis in the presence of nocodazole (100 nM and 250 nM), cortical dynein enrichment was impaired in a dose-dependent manner (Fig. 2B–D). In 100 nM nocodazole, small patches of dynein-enriched areas were observed at random cortical regions, whereas enrichment was completely abolished in cells treated at a nocodazole concentration of 250 nM (Fig. 2C, D, and F). Nonetheless, the initial symmetric recruitment of dynein to the cortex still took place, albeit with lower efficiency under the detection limit of the macro (Fig. S2B). This might indicate a highly transient cortical recruitment of dynein that is dependent on extracellular cues, which needs subsequent stabilization by microtubules that are nucleated upon NEB. When cells entered mitosis in the presence of nocodazole, and subsequently were allowed to re-polymerize spindle microtubules by nocodazole washout into new media containing the Eg5 inhibitor STLC, the KT pool of dynein persisted, and cortical dynein enrichment was re-established to a level comparable to untreated control cells (Fig. S3A–C; Fig. 2G). Thus, the defect in cortical dynein enrichment seen after treatment with spindle poisons occurs independent of the sustained KT–dynein localization caused by persistent absence of stable KT–microtubule attachments.^{51,52}

Conversely, when cells were treated with a low dose of the microtubule-stabilizing agent taxol (1.5 nM), dynein was properly enriched at cortical regions near the short edge of the rectangular micropattern immediately after mitotic entry (Fig. 2E). During the mitotic arrest, however, cortical dynein enrichment sites became randomized (Fig. 2E and F), presumably because the spindle started to rotate and/or due to disorganization of the mitotic spindle. Taken together, these data indicate that spindle microtubules are required for continued recruitment of cortical dynein to the cell cortex. Notably, the overall cortical dynein enrichment level in cells with taxol-stabilized spindles was comparable to control untreated cells (Fig. 2G), suggesting that dynein enrichment does not require dynamic microtubules.

Astral microtubules determine the sites of cortical dynein enrichment

In order to specifically address the role of astral microtubules in cortical dynein enrichment, we set up an assay in which we could selectively modulate the stability of the astrals without affecting the other population of the spindle microtubules. Kif18b is a member of the kinesin-8 family that possesses microtubule depolymerizing activity. Kif18b was shown to localize to the plus-ends of astral microtubules and was found to specifically affect the dynamics and stability of astral microtubules.^{53,54} Despite affecting spindle dynamics at the astral tips, Kif18b depletion does not cause major defects in bipolar spindle organization, and cells are

capable of progressing normally through mitosis.⁵³ Consistently, we did not observe any obvious defects in spindle morphology when live-cell imaging was performed with H2B-RFP and GFP-tubulin co-expressing cells transfected with siRNA against Kif18b (Fig. S4A). Western blot analysis confirmed the efficiency of our siRNA-mediated depletion of Kif18b (Fig. S4B). Importantly, Kif18b knockdown caused spindle misorientation in cells plated on the rectangular micropattern (Fig. 3A). The randomly assumed centrosome positions at the time of NEB were maintained throughout mitosis in Kif18b-depleted cells, and the spindle did not rotate into the correct angle relative to the shape (Fig. 3B and C). We then went on to test the effect of the spindle misorientation on cortical dynein localization by interfering with Kif18b expression in the DHC-GFP-expressing cell line. We found that the initial recruitment of dynein to the cortex was unaffected when compared with GAPDH-depleted control cells (Fig. 3B and C). However, as cells progressed further through mitosis, dynein-enriched sites did not remain restricted to the cortical areas at 45°–135° or 225°–315°, but shifted toward cortical regions that contact most of the astral microtubules of the misoriented spindle (Fig. 3C). By the time cells reached metaphase, dynein enrichment sites were dominated by the position of the misoriented spindle and displayed random localization relative to the shape (Fig. 3D). These observations further support a role of astral microtubules in cortical dynein targeting.

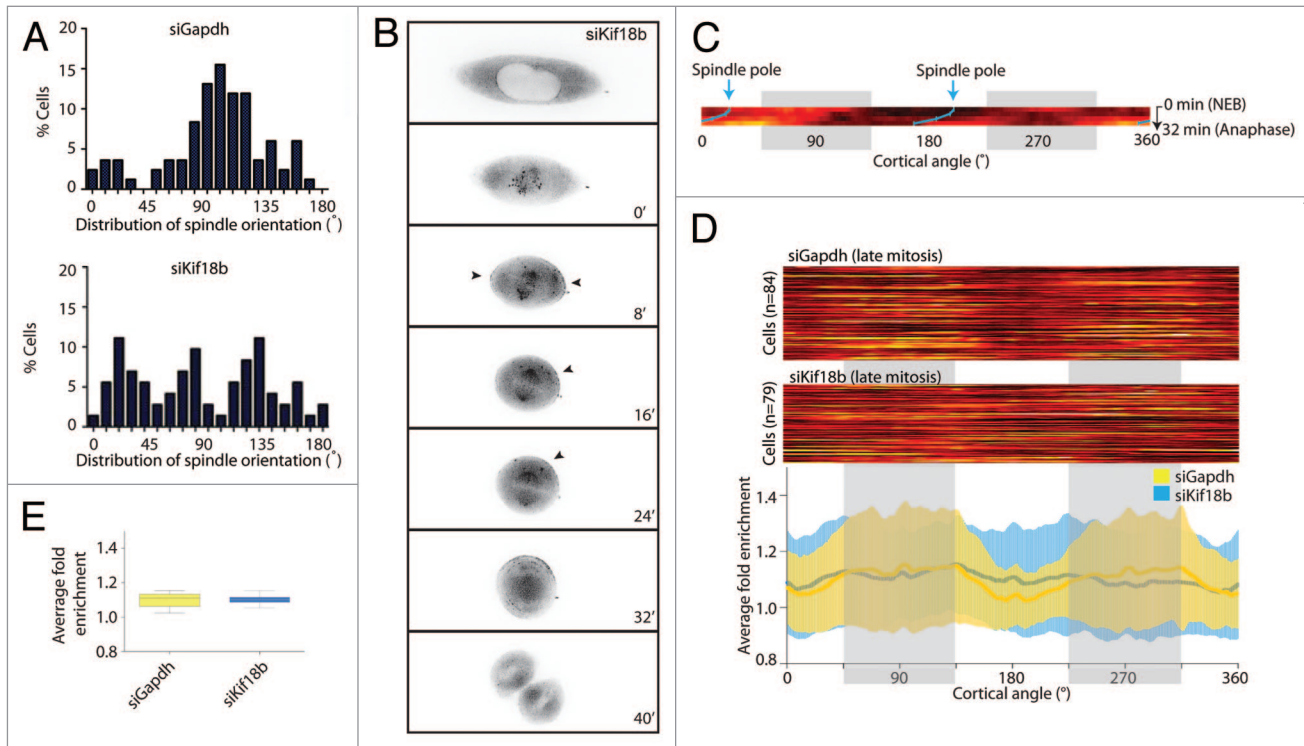


Figure 3. Astral microtubules determine sites of cortical dynein enrichment. **(A)** Distributions of spindle orientation at late mitotic time points in control GAPDH-depleted (top) and Kif18b-depleted cells (bottom). Data are extracted from 2 independent experiments per condition. **(B)** A micropatterned DHC-GFP HeLa cell treated with Kif18b-specific siRNA for 48 h exhibits spindle misorientation. Time is relative to NEB. **(C)** Kymograph of cortical dynein enrichment extracted from the example cell in **(B)**. The angles of the mitotic spindle relative to the shape are plotted at corresponding time points (blue line). **(D)** Heatmaps (top) and quantification (bottom) of cortical DHC-GFP enrichment obtained from the experiments shown in **(A)**. **(E)** Quantification of average DHC-GFP enrichment in **(D)** plotted as a box plot.

Discussion

A large body of evidence indicates that polarization of the mitotic cell body, which eventually dictates spindle orientation, depends on the cell's contacts with its adhesive microenvironment³⁹⁻⁴¹ (Fig. 1). This suggests that extracellular factors are determinants for the (initial) sites of cortical dynein enrichment in mitosis. The molecular mechanism of how these extracellular cues are linked to cortical dynein recruitment remains elusive. In yeast, it is clear that there are no extracellular cues that dictate spindle orientation, thus polarization of the cell body occurs through a cell-intrinsic pathway.⁵⁵ Spindle orientation along the polarity axis in yeast critically depends on the function of dynein, and astral microtubules play key functions in dynein's cortical targeting pathway. Through high-resolution live cell microscopy, single dynein molecules were observed while being offloaded from bundled astral microtubules to the cell cortex.^{32,33} While reports of astral microtubule localization of dynein components have been made utilizing fixed assays in some mammalian systems,⁵⁶ the involvement of astral microtubules in cortical dynein targeting has never been carefully explored.

Here, we have manipulated (astral) microtubule stability using a number of different approaches, and find that astral microtubules are required for localized dynein recruitment to the cortex and can be a determining factor for cortical dynein enrichment sites in mitosis. A number of previous studies have reported that de-stabilization of astral microtubules by low-dose nocodazole treatments have no effect²⁰ or even a positive effect on cortical dynein localization, where new cortical regions become occupied with dynein upon nocodazole treatment.⁵⁷ In addition, another study reported that cortical LGN localization becomes enhanced upon nocodazole treatment, suggesting that astral microtubules are required for the proper turnover of LGN toward the spindle poles.⁵⁸ Indeed, we also find that a substantial fraction of cells (>65%) display dynein at the cortex when asynchronous populations are treated with a high dose of nocodazole, and we observed a minor increase in the fraction of cells where the cortical dynein crescent appeared diffuse and covering a larger area of the cortex (Fig. 2A; 4% in control, 12% and 11% at 100 nM and 250 nM nocodazole, respectively), indicating that dynein has low turnover at the cortex when microtubules are depolymerized in mitotically arrested cells. However, through live-cell imaging we find that nocodazole-treated cells fail to sustain the dynamic asymmetric distribution of cortical dynein. On the contrary, treatment with taxol does not result in a loss of dynein from the cell cortex. Rather it leads to perturbation of the asymmetric distribution of dynein. Moreover, depletion of the microtubule-destabilizing kinesin Kif18b results in spindle misorientation, which, in turn, over time causes the deposition of dynein at cortical sites that do not correspond to the initial recruitment site (Fig. 3B and C). Combined, these data suggest that astral microtubules have a positive effect on cortical dynein localization, and that it is required for the sustained localized enrichment of dynein. However, the level of dynein enrichment at the cortex is not affected in the taxol-treated or Kif18b-depleted cells (Figs. 2G and 3E), although microtubule dynamics are severely

compromised. This suggests that the presence of polymerized tubulins is sufficient to promote dynein recruitment to the cortex.

Our data show that initial recruitment of dynein to the cortex is dictated by the geometry of cell adhesion. Following the initial recruitment phase, we find that further recruitment of dynein to the cortex depends on astral microtubules. Possibly, a plus-end-directed motor transports dynein to cortical sites where it is allowed to anchor to its upstream factors NuMA/LGN/G α i. Alternatively, dynein is stabilized at the cell cortex whenever astral microtubules are present. It is not unlikely that the astral microtubules themselves function to deposit dynein at the cortex, allowing them to quickly generate a pulling force on the spindle that helps to establish the proper orientation. In the cells grown on a micropattern, initial recruitment of dynein is largely dictated by the geometry of adhesion, causing dynein to accumulate on opposing sides of the cell along the short axis of the cell. This pool of dynein can function as the initial force-generating platform to orient the spindle, such that the majority of astral microtubules will meet the cortex at the sites of initial dynein recruitment. This 2-step mechanism can further enforce spindle orientation along the long axis of the cell. As mentioned above, recruitment of dynein to the cell cortex is negatively regulated by chromosome- and centrosome-derived signals. This superimposes an additional level of control over cortical dynein dynamics that allows selective recruitment of dynein to cortical sites that are not in close proximity of the spindle poles or the chromosomes. Combined, these mechanisms provide all the ingredients to allow a cell to position the spindle in the center of the cell, aligned with its geometry of cell adhesion.

In summary, we have revealed a role for dynein in linking extracellular cues to spindle orientation in cells undergoing cell division under geometric constraints. Furthermore, our data indicate a function for astral microtubules in cortical dynein targeting in the mammalian system. It will be of great interest for the future to resolve the molecular link between the extracellular and intracellular pathways of cortical dynein recruitment, and how these 2 pathways might interplay or be differentially activated in different cell types.

Materials and Methods

Cell culture and siRNA transfection

HeLa and U2OS cells were maintained in DMEM (Gibco) supplemented with 6% FCS, 100 U/ml penicillin, and 100 μ g/ml streptomycin. HeLa cells expressing mouse DHC-GFP were obtained from MitoCheck⁴⁷ and further clonally propagated after fluorescent cell sorting of single cells. For drug treatments, cells were incubated with respective drugs at the following concentrations: Nocodazole, 100, 250, or 500 nM; Taxol, 1.5 nM (depicted in each figure); STLC, 20 μ M; MG-132, 20 μ M; Thymidine, 2 mM. RNAi experiments were conducted using Lipofectamine RNAi MAX transfection reagent (LifeTechnologies) according to the manufacturer's guidelines. We used previously validated pools of 4 pre-designed siRNA oligonucleotides against human LGN/GPSM2,²⁰ Kif18b,⁵³ and GAPDH.⁵⁹ All siRNA transfections were performed 48 h prior to the start of the experiments.

Immunofluorescence and microscopy

For live-cell imaging of micropatterned cells, cells were synchronized at the G₁/S-phase using a single thymidine block for 24 h and then removed from the dish by trypsinization. Cells were re-suspended in fresh media and deposited on the micropatterned coverslip at a density of 3×10^4 cells/cm². For live-cell imaging, the media was replaced with Leibowitz L15 CO₂-independent medium and maintained in a heated chamber at 37 °C. Images were taken every 8 min with a microscope (Deltavision Elite; Applied Precision) equipped with a Coolsnap HQ2 camera. Seven z-sections were acquired at 2.1- μ m intervals using a PlanApo N 60 \times /NA 1.42 objective (Olympus). Equivalent exposure conditions and scaling were used in each experiment. Images were deconvolved using the DeltaVision software. Images were generated by maximum intensity projection of entire cells and analyzed using ImageJ software (National Institutes of Health).

For immunofluorescence experiments, cells were pre-extracted in PEM buffer (0.1 M PIPES pH 6.8, 2 mM EGTA, 1 mM MgCl₂, 0.1% Triton X-100) for 1 min and fixed in the same buffer containing 4% paraformaldehyde for 10 min. For immunostaining, anti- α -tubulin (Sigma) was used at 1:10000. The primary antibody was incubated overnight at 4 °C and secondary antibodies (Alexa-488 and Phalloidin-Alexa-561, Molecular Probes) were incubated for 2 h at room temperature. The same microscope set-up was used as described above for live-cell imaging. Thirty–40 images were acquired at 200-nm intervals. Equivalent exposure conditions and scaling was used in each experiment. Images were deconvolved using the DeltaVision software. Images were generated by maximum intensity projection of entire cells. Brightness and contrast were adjusted with ImageJ software.

Micropatterning on glass

The photomask was custom-made (Delta Mask) and was printed with rectangular shapes with a dimension of 20 μ m \times 80 μ m. Adhesive fibronectin micropatterns were produced using deep-UV illumination through a photomask according to a previously described protocol.⁶⁰

Measure of cortical dynein enrichment

We developed an ImageJ macro that was able to automatically detect a fluorescent cell on a micropattern. The boundaries of DHC-GFP-expressing cells were detected through the Otsu dark thresholding method. Subsequently, edge detection was applied

for creating outlines for the linescan measurement. The center of the round mitotic cell, defined as a centroid center, was used to set the position of the linescan. The linescan measured intensity values around the cell perimeter at a width of 5 pixels in clockwise direction, starting from the highest centroid position. The moment of mitotic rounding and anaphase onset was detected by recording the centroid's roundness, defined by its x - y ratio. The cell roundness threshold was set to 0.7, above which the macro recorded linescan measurements throughout the time-lapse images. The macro generated relative values of GFP intensities by dividing the 5-pixels mean value at each measurement point with the modal value recorded for the whole linescan at individual time frames. Relative intensity values were used for generating heatmaps of 1-pixel height and 360-pixel width for each time frame. Each heatmap was scaled equally.

Western blotting

Cells were transfected with indicated siRNAs for 48 h. Mitotic cells were harvested after an overnight treatment with 20 μ M STLC and lysed with Laemmli buffer (120 mM Tris, pH 6.8, 4% SDS, and 20% glycerol). Protein concentration was determined by the Lowry method, and equal amounts were separated on a poly-acrylamide gel. After transfer to nitrocellulose membranes, the blots were probed with the following antibodies: anti- α -tubulin (1:1000; Sigma) and anti-Kif18b (1:200;⁵³). HRP-conjugated secondary antibodies (Dako) were used in a 1:2000 dilution.

Disclosure of Potential Conflicts of Interest

No potential conflicts of interest were disclosed.

Acknowledgments

We thank Rob Klompaker for maintaining the microscopes, Ina Poser, and Anthony A Hyman for the HeLa DHC-GFP cell line and Daniel W Gerlich for the HeLa GFP- α -tubulin RFP-H2B cell line. Furthermore, we thank members of the Medema, Rowland and Wolhuis groups for helpful discussions. R.H.M. was supported by the ZonMw TOP grant (UU-code R2010).

Supplemental Materials

Supplemental materials may be found here: www.landesbioscience.com/journals/cc/article/28031

References

1. Glotzer M. The mechanism and control of cytokinesis. *Curr Opin Cell Biol* 1997; 9:815-23; PMID:9425346; [http://dx.doi.org/10.1016/S0955-0674\(97\)80082-8](http://dx.doi.org/10.1016/S0955-0674(97)80082-8)
2. Pearson CG, Bloom K. Dynamic microtubules lead the way for spindle positioning. *Nat Rev Mol Cell Biol* 2004; 5:481-92; PMID:15173827; <http://dx.doi.org/10.1038/nrm1402>
3. Gönczy P. Mechanisms of asymmetric cell division: flies and worms pave the way. *Nat Rev Mol Cell Biol* 2008; 9:355-66; PMID:18431399; <http://dx.doi.org/10.1038/nrm2388>
4. Knoblich JA. Asymmetric cell division: recent developments and their implications for tumour biology. *Nat Rev Mol Cell Biol* 2010; 11:849-60; PMID:21102610; <http://dx.doi.org/10.1038/nrm3010>
5. Morin X, Bellaïche Y. Mitotic spindle orientation in asymmetric and symmetric cell divisions during animal development. *Dev Cell* 2011; 21:102-19; PMID:21763612; <http://dx.doi.org/10.1016/j.devcel.2011.06.012>
6. Desai A, Mitchison TJ. Microtubule polymerization dynamics. *Annu Rev Cell Dev Biol* 1997; 13:83-117; PMID:9442869; <http://dx.doi.org/10.1146/annurev.cellbio.13.1.83>
7. Howard J, Hyman AA. Dynamics and mechanics of the microtubule plus-end. *Nature* 2003; 422:753-8; PMID:12700769; <http://dx.doi.org/10.1038/nature01600>
8. Grill SW, Hyman AA. Spindle positioning by cortical pulling forces. *Dev Cell* 2005; 8:461-5; PMID:15809029; <http://dx.doi.org/10.1016/j.devcel.2005.03.014>
9. Minc N, Burgess D, Chang F. Influence of cell geometry on division-plane positioning. *Cell* 2011; 144:414-26; PMID:21295701; <http://dx.doi.org/10.1016/j.cell.2011.01.016>
10. Grill SW, Gönczy P, Stelzer EH, Hyman AA. Polarity controls forces governing asymmetric spindle positioning in the *Caenorhabditis elegans* embryo. *Nature* 2001; 409:630-3; PMID:11214323; <http://dx.doi.org/10.1038/35054572>
11. Grill SW, Howard J, Schäffer E, Stelzer EH, Hyman AA. The distribution of active force generators controls mitotic spindle position. *Science* 2003; 301:518-21; PMID:12881570; <http://dx.doi.org/10.1126/science.1086560>
12. Redemann S, Pecreaux J, Goehring NW, Khairy K, Stelzer EHK, Hyman AA, Howard J. Membrane invaginations reveal cortical sites that pull on mitotic spindles in one-cell *C. elegans* embryos. *PLoS One* 2010; 5:e12301; PMID:20808841; <http://dx.doi.org/10.1371/journal.pone.0012301>
13. Carminati JL, Stearns T. Microtubules orient the mitotic spindle in yeast through dynein-dependent interactions with the cell cortex. *J Cell Biol* 1997; 138:629-41; PMID:9245791; <http://dx.doi.org/10.1083/jcb.138.3.629>

14. Adames NR, Cooper JA. Microtubule interactions with the cell cortex causing nuclear movements in *Saccharomyces cerevisiae*. *J Cell Biol* 2000; 149:863-74; PMID:10811827; <http://dx.doi.org/10.1083/jcb.149.4.863>
15. Heil-Chapdelaine RA, Oberle JR, Cooper JA. The cortical protein Num1p is essential for dynein-dependent interactions of microtubules with the cortex. *J Cell Biol* 2000; 151:1337-44; PMID:11121446; <http://dx.doi.org/10.1083/jcb.151.6.1337>
16. Gönczy P, Pichler S, Kirkham M, Hyman AA. Cytoplasmic dynein is required for distinct aspects of MTOC positioning, including centrosome separation, in the one cell stage *Caenorhabditis elegans* embryo. *J Cell Biol* 1999; 147:135-50; PMID:10508861; <http://dx.doi.org/10.1083/jcb.147.1.135>
17. Couwenbergs C, Labbé JC, Goulding M, Marty T, Bowerman B, Gotta M. Heterotrimeric G protein signaling functions with dynein to promote spindle positioning in *C. elegans*. *J Cell Biol* 2007; 179:15-22; PMID:17908918; <http://dx.doi.org/10.1083/jcb.200707085>
18. Nguyen-Ngoc T, Afshar K, Gönczy P. Coupling of cortical dynein and G α proteins mediates spindle positioning in *Caenorhabditis elegans*. *Nat Cell Biol* 2007; 9:1294-302; PMID:17922003; <http://dx.doi.org/10.1038/ncb1649>
19. Williams SE, Beronja S, Pasolli HA, Fuchs E. Asymmetric cell divisions promote Notch-dependent epidermal differentiation. *Nature* 2011; 470:353-8; PMID:21331036; <http://dx.doi.org/10.1038/nature09793>
20. Kiyomitsu T, Cheeseman IM. Chromosome- and spindle-pole-derived signals generate an intrinsic code for spindle position and orientation. *Nat Cell Biol* 2012; 14:311-7; PMID:22327364; <http://dx.doi.org/10.1038/ncb2440>
21. Kotak S, Busso C, Gönczy P. Cortical dynein is critical for proper spindle positioning in human cells. *J Cell Biol* 2012; 199:97-110; PMID:23027904; <http://dx.doi.org/10.1083/jcb.201203166>
22. Schroer TA. Dynactin. *Annu Rev Cell Dev Biol* 2004; 20:759-79; PMID:15473859; <http://dx.doi.org/10.1146/annurev.cellbio.20.012103.094623>
23. Kardon JR, Vale RD. Regulators of the cytoplasmic dynein motor. *Nat Rev Mol Cell Biol* 2009; 10:854-65; PMID:19935668; <http://dx.doi.org/10.1038/nrm2804>
24. Raaijmakers JA, Tanenbaum ME, Medema RH. Systematic dissection of dynein regulators in mitosis. *J Cell Biol* 2013; 201:201-15; PMID:23589491; <http://dx.doi.org/10.1083/jcb.201208098>
25. Kikkawa M. Big steps toward understanding dynein. *J Cell Biol* 2013; 202:15-23; PMID:23836927; <http://dx.doi.org/10.1083/jcb.201304099>
26. Dujardin DL, Vallee RB. Dynein at the cortex. *Curr Opin Cell Biol* 2002; 14:44-9; PMID:11792543; [http://dx.doi.org/10.1016/S0955-0674\(01\)00292-7](http://dx.doi.org/10.1016/S0955-0674(01)00292-7)
27. Laan L, Pavin N, Husson J, Romet-Lemonne G, van Duijn M, López MP, Vale RD, Jülicher F, Reck-Peterson SL, Dogterom M. Cortical dynein controls microtubule dynamics to generate pulling forces that position microtubule asters. *Cell* 2012; 148:502-14; PMID:22304918; <http://dx.doi.org/10.1016/j.cell.2012.01.007>
28. Laan L, Roth S, Dogterom M. End-on microtubule-dynein interactions and pulling-based positioning of microtubule organizing centers. *Cell Cycle* 2012; 11:3750-7; PMID:22895049; <http://dx.doi.org/10.4161/cc.21753>
29. Markus SM, Lee W-L. Microtubule-dependent path to the cell cortex for cytoplasmic dynein in mitotic spindle orientation. *Bioarchitecture* 2011; 1:209-15; PMID:22754610; <http://dx.doi.org/10.4161/bioa.18103>
30. Sheeman B, Carvalho P, Sagot I, Geiser J, Kho D, Hoyt MA, Pellman D. Determinants of *S. cerevisiae* dynein localization and activation: implications for the mechanism of spindle positioning. *Curr Biol* 2003; 13:364-72; PMID:12620184; [http://dx.doi.org/10.1016/S0960-9822\(03\)00013-7](http://dx.doi.org/10.1016/S0960-9822(03)00013-7)
31. Markus SM, Punch JJ, Lee W-L. Motor- and tail-dependent targeting of dynein to microtubule plus-ends and the cell cortex. *Curr Biol* 2009; 19:196-205; PMID:19185494; <http://dx.doi.org/10.1016/j.cub.2008.12.047>
32. Markus SM, Lee W-L. Regulated offloading of cytoplasmic dynein from microtubule plus-ends to the cortex. *Dev Cell* 2011; 20:639-51; PMID:21571221; <http://dx.doi.org/10.1016/j.devcel.2011.04.011>
33. Ananthanarayanan V, Schattat M, Vogel SK, Krull A, Pavin N, Tolić-Nørrelykke IM. Dynein motion switches from diffusive to directed upon cortical anchoring. *Cell* 2013; 153:1526-36; PMID:23791180; <http://dx.doi.org/10.1016/j.cell.2013.05.020>
34. Du Q, Macara IG. Mammalian Pins is a conformational switch that links NuMA to heterotrimeric G proteins. *Cell* 2004; 119:503-16; PMID:15537540; <http://dx.doi.org/10.1016/j.cell.2004.10.028>
35. Kotak S, Busso C, Gönczy P. Cortical dynein is critical for proper spindle positioning in human cells. *J Cell Biol* 2012; 199:97-110; PMID:23027904; <http://dx.doi.org/10.1083/jcb.201203166>
36. Kiyomitsu T, Cheeseman IM. Cortical dynein and asymmetric membrane elongation coordinately position the spindle in anaphase. *Cell* 2013; 154:391-402; PMID:23870127; <http://dx.doi.org/10.1016/j.cell.2013.06.010>
37. Kotak S, Busso C, Gönczy P. NuMA phosphorylation by CDK1 couples mitotic progression with cortical dynein function. *EMBO J* 2013; 32:2517-29; PMID:23921553; <http://dx.doi.org/10.1038/emboj.2013.172>
38. Kotak S, Gönczy P. NuMA phosphorylation dictates dynein-dependent spindle positioning. *Cell Cycle* 2014; 13:177-8; PMID:24241204; <http://dx.doi.org/10.4161/cc.27040>
39. Théry M, Racine V, Pépin A, Piel M, Chen Y, Sibarita J-B, Bornens M. The extracellular matrix guides the orientation of the cell division axis. *Nat Cell Biol* 2005; 7:947-53; PMID:16179950; <http://dx.doi.org/10.1038/ncb1307>
40. Théry M, Jiménez-Dalmaroni A, Racine V, Bornens M, Jülicher F. Experimental and theoretical study of mitotic spindle orientation. *Nature* 2007; 447:493-6; PMID:17495931; <http://dx.doi.org/10.1038/nature05786>
41. Fink J, Carpi N, Betz T, Bétard A, Chebah M, Azzioune A, Bornens M, Sykes C, Fetler L, Cuvelier D, et al. External forces control mitotic spindle positioning. *Nat Cell Biol* 2011; 13:771-8; PMID:21666685; <http://dx.doi.org/10.1038/ncb2269>
42. Zhu M, Settle F, Kotak S, Sanchez-Pulido L, Ehret L, Ponting CP, Gönczy P, Hoffmann I. MISP is a novel Plk1 substrate required for proper spindle orientation and mitotic progression. *J Cell Biol* 2013; 200:773-87; PMID:23509069; <http://dx.doi.org/10.1083/jcb.201207050>
43. Maier B, Kirsch M, Anderhub S, Zentgraf H, Krämer A. The novel actin/focal adhesion-associated protein MISP is involved in mitotic spindle positioning in human cells. *Cell Cycle* 2013; 12:1457-71; PMID:23574715; <http://dx.doi.org/10.4161/cc.24602>
44. Kaji N, Muramoto A, Mizuno K. LIM kinase-mediated cofilin phosphorylation during mitosis is required for precise spindle positioning. *J Biol Chem* 2008; 283:4983-92; PMID:18079118; <http://dx.doi.org/10.1074/jbc.M708644200>
45. Mitsushima M, Toyoshima F, Nishida E. Dual role of Cdc42 in spindle orientation control of adherent cells. *Mol Cell Biol* 2009; 29:2816-27; PMID:19273597; <http://dx.doi.org/10.1128/MCB.01713-08>
46. Toyoshima F, Matsumura S, Morimoto H, Mitsushima M, Nishida E. PtdIns(3,4,5)P₃ regulates spindle orientation in adherent cells. *Dev Cell* 2007; 13:796-811; PMID:18061563; <http://dx.doi.org/10.1016/j.devcel.2007.10.014>
47. Poser I, Sarov M, Hutchins JRA, Hériché J-K, Toyoda Y, Pozniakovskiy A, Weigl D, Nitzsche A, Hegemann B, Bird AW, et al. BAC TransgeneOmics: a high-throughput method for exploration of protein function in mammals. *Nat Methods* 2008; 5:409-15; PMID:18391959; <http://dx.doi.org/10.1038/nmeth.1199>
48. Heald R, Tournebise R, Blank T, Sandaltzopoulos R, Becker P, Hyman A, Karsenti E. Self-organization of microtubules into bipolar spindles around artificial chromosomes in *Xenopus* egg extracts. *Nature* 1996; 382:420-5; PMID:8684481; <http://dx.doi.org/10.1038/382420a0>
49. Goshima G, Nédélec F, Vale RD. Mechanisms for focusing mitotic spindle poles by minus-end-directed motor proteins. *J Cell Biol* 2005; 171:229-40; PMID:16247025; <http://dx.doi.org/10.1083/jcb.200505107>
50. Corrigan AM, Shrestha RL, Zulkli I, Hiroi N, Liu Y, Tamura N, Yang B, Patel J, Funahashi A, Donald A, et al. Automated tracking of mitotic spindle pole positions shows that LGN is required for spindle rotation but not orientation maintenance. *Cell Cycle* 2013; 12:2643-55; PMID:23907121; <http://dx.doi.org/10.4161/cc.25671>
51. Tai CY, Dujardin DL, Faulkner NE, Vallee RB. Role of dynein, dynactin, and CLIP-170 interactions in LIS1 kinetochore function. *J Cell Biol* 2002; 156:959-68; PMID:11889140; <http://dx.doi.org/10.1083/jcb.200109046>
52. Vergnolle MAS, Taylor SS. Cenp-F links kinetochores to Ndel1/Nde1/Lis1/dynein microtubule motor complexes. *Curr Biol* 2007; 17:1173-9; PMID:17600710; <http://dx.doi.org/10.1016/j.cub.2007.05.077>
53. Tanenbaum ME, Macérek L, van der Vaart B, Galli M, Akhmanova A, Medema RH. A complex of Kif18b and MCAK promotes microtubule depolymerization and is negatively regulated by Aurora kinases. *Curr Biol* 2011; 21:1356-65; PMID:21820309; <http://dx.doi.org/10.1016/j.cub.2011.07.017>
54. Stout JR, Yount AL, Powers JA, Leblanc C, Ems-McClung SC, Walczak CE. Kif18B interacts with EB1 and controls astral microtubule length during mitosis. *Mol Biol Cell* 2011; 22:3070-80; PMID:21737685; <http://dx.doi.org/10.1091/mbc.E11-04-0363>
55. Siller KH, Doe CQ. Spindle orientation during asymmetric cell division. *Nat Cell Biol* 2009; 11:365-74; PMID:19337318; <http://dx.doi.org/10.1038/ncb0409-365>
56. Busson S, Dujardin D, Moreau A, Dompierre J, De Mey JR. Dynein and dynactin are localized to astral microtubules and at cortical sites in mitotic epithelial cells. *Curr Biol* 1998; 8:541-4; PMID:9560347; [http://dx.doi.org/10.1016/S0960-9822\(98\)70208-8](http://dx.doi.org/10.1016/S0960-9822(98)70208-8)
57. Collins ES, Balchand SK, Faraci JL, Wadsworth P, Lee WL. Cell cycle-regulated cortical dynein/dynactin promotes symmetric cell division by differential pole motion in anaphase. *Mol Biol Cell* 2012; 23:3380-90; PMID:22809624; <http://dx.doi.org/10.1091/mbc.E12-02-0109>
58. Zheng Z, Wan Q, Liu J, Zhu H, Chu X, Du Q. Evidence for dynein and astral microtubule-mediated cortical release and transport of Gai/LGN/NuMA complex in mitotic cells. *Mol Biol Cell* 2013; 24:901-13; PMID:23389635; <http://dx.doi.org/10.1091/mbc.E12-06-0458>
59. Raaijmakers JA, van Heesbeen RGHP, Meaders JL, Geers EF, Fernandez-Garcia B, Medema RH, Tanenbaum ME. Nuclear envelope-associated dynein drives prophase centrosome separation and enables Eg5-independent bipolar spindle formation. *EMBO J* 2012; 31:4179-90; PMID:23034402; <http://dx.doi.org/10.1038/emboj.2012.272>
60. Azzioune A, Storch M, Bornens M, Théry M, Piel M. Simple and rapid process for single cell micro-patterning. *Lab Chip* 2009; 9:1640-2; PMID:19458875; <http://dx.doi.org/10.1039/b821581m>